Chapter 1

Learning from Nature: Unsteady Flow Physics in Bioinspired Flapping Flight

Haibo Dong, Ayodeji T. Bode-Oke and Chengyu Li

Additional information is available at the end of the chapter

http://dx.doi.org/10.5772/intechopen.73091

Abstract

There are few studies on wing flexibility and the associated aerodynamic performance of insect wings during free flight, which are potential candidates for developing bioinspired microaerial vehicles (MAVs). To this end, this chapter aims at understanding wing deformation and motions of insects through a combined experimental and computational approach. Two sets of techniques are currently being developed to make this integration possible: first, data acquisition through the use of high-speed photogrammetry and accurate data reconstruction to quantify the wing and body motions in free flight with great detail and second, direct numerical simulation (DNS) for force measurements and visualization of vortex structures. Unlike most previous studies that focus on the near-field vortex formation mechanisms of a single rigid flapping wing, this chapter presents freely flying insects with full-field vortex structures and associated unsteady aerodynamics at low Reynolds numbers. Our chapter is expected to lead to valuable insights into the underlying physics about flow mechanisms of low Reynolds number flight in nature, which will have great significance to flapping-wing MAV design and optimization research in the future.

Keywords: insect flight, high-speed photogrammetry, wing kinematics, wing flexibility, unsteady aerodynamics

1. Introduction

In nature, flying is a unique mechanism for generating control and maneuvering forces by flapping the wings. Weis-Fogh and Jensen [1] described flapping flight as a complex physical and biological problem that it is impossible to understand a single part of the process completely. One of the reasons is that the unsteady motion of wings has related flow mechanisms at a Reynolds number (Re) of 10 to 10^5 [2]. **Figure 1** illustrates a trend in the relationship between

the Reynolds number and the body mass of both natural and man-made flying subjects. At this flow regime, lift producing mechanisms are intrinsically unsteady and vortex-dominated. Spanning over decades, considerable progress in understanding flapping flight has been achieved, and some general unsteady mechanisms have been identified. Examples include clap-and-fling [3–7], leading-edge vortex (LEV) [8–11], rotational lift [8, 12], wake capture [8, 13], wing-wing interactions, and body-wing interactions [14]. By using the rigid wing assumption, many of these mechanisms could explain the fluid phenomena near the wing, which are expressed as the motion of vortices, as well as the instantaneously local and resultant forces.

Flapping flight is a mode of transport widely adopted by natural fliers and has captured the interests of biologists and engineers because of several unique characteristics. From an energetic perspective, the propulsive efficiency of flapping motion can be higher than 85% [15]. Hence, flapping flight can be chosen as an alternative solution for aircraft propulsion to meet the need for high efficiency in energy consumption [16]. From the perspective of maneuverability and controllability, birds and insects have shown remarkable flying capabilities in tight spaces with multiple obstacles. In contrast, conventional aircraft cannot operate in such circumstances. The advantages of flapping flight have led to the development of micro air vehicles (MAVs) which mimic flapping flight. Many aspects of flapping flight, such as wing kinematics, structural response of wing, power consumption, and aerodynamics, are worth exploring. In particular, from a fluid dynamic point of view, the interaction of the flapping appendages with the surrounding air leads to the generation of vortices. Studying these vortex structures is of great importance for two reasons.

First, the vortex formation is related to the aerodynamic force, either indirectly or directly. Exerting forces on fluids can deform the fluids and leave footprints of the propulsion in the wake [17]. Therefore, even without force sensors and directly measuring pressure field, some elementary conclusions on force generation can be drawn based on the observed vortex formation in

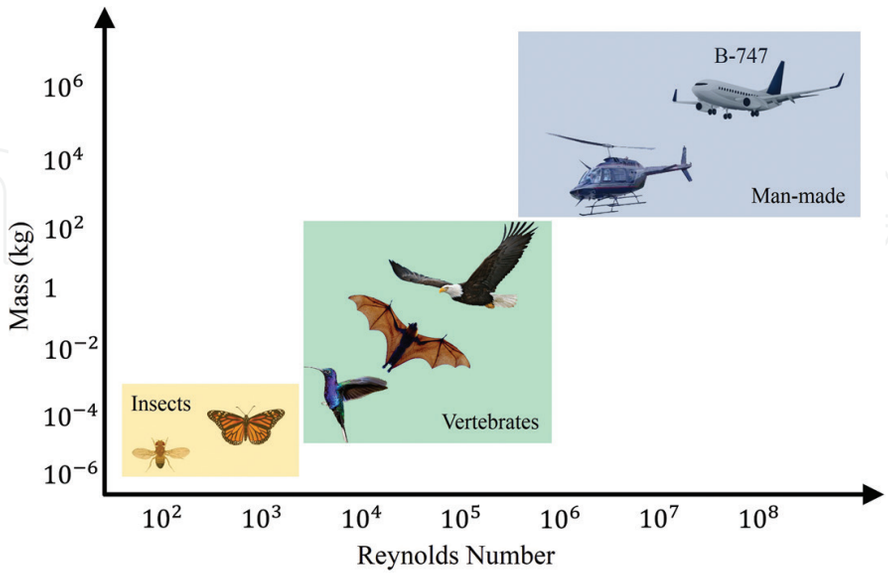

Figure 1. Characteristics of biological flapping flight and conventional man-made flight based on the Reynolds number and body mass. Picture courtesy of Science & Society Picture Library.

the wake. For example, it has been shown by [18] that the location and orientation of vortex streets behind an oscillating airfoil can indicate if the force acting on the airfoil is drag-indicative or thrust-indicative. When sufficient velocity and vorticity information around a submerged body is given, the wake survey methods can accurately predict force acting on the body [19–21]. Because force exerted by fluids on an immersed body is equal and opposite to the force exerted by the body to the fluids, controlling the vortex shedding in the wake of an airfoil is found to be effective in changing the aerodynamic performance of the airfoil [22].

Second, flapping flight usually operates in a low *Re* regime, and many of flow phenomena can be readily explained by using vortex dynamics. According to the well-known Biot-Savart law, vortex structures in far field can induce velocity change near a flapping wing without direct interaction. Tijdeman and Seebass [23] present an example of how vorticity in downstream induced velocity around an airfoil and caused the oscillation of lift lag behind the motion of the airfoil. A few but important near-field mechanisms for lift enhancement, that is, leading edge vortex [24], rotational forces, and wake capture [8], have also accounted for the presence of vortex structures and their interactions with flapping wings.

1.1. Insect wing and its motion

Insect wings are thin cuticular structures enforced by veins that spread across the wing in intricate patterns. The leading edge of the wing contains thickened veins that provide structural rigidity. These several radially stretched flexion lines on the wing represent regions of increased flexibility along which the wing can deform and yield variable camber [25]. Using a dragonfly forewing as an example, **Figure 2** shows the leading edge of the wing is enforced by multiple vein structures. Wing mass mostly arises from the wing venation, and the pattern of the wing venation varies among species with the wing to body mass ratio ranging between 0.5–4% in dipterans and hymenopterans and 3–10% in butterflies [26, 27].

The distribution of the wing mass has mechanical importance. Spanwise mass distribution defines the wing's moment of inertia about its hinge point and therefore indicates the power required for flapping the wings. The center of mass (CoM) of the insect wings usually lies at about 30–40% of the wing length from the wing hinge, reducing the wing moment of inertia. The chordwise distribution of the wing mass also is important in easing wing rotation at stroke reversal. The wing's center of mass is located below the longitudinal axis of rotation of the wing. Therefore, the inertial forces due to the wing acceleration help flip the wing at the stroke reversal.

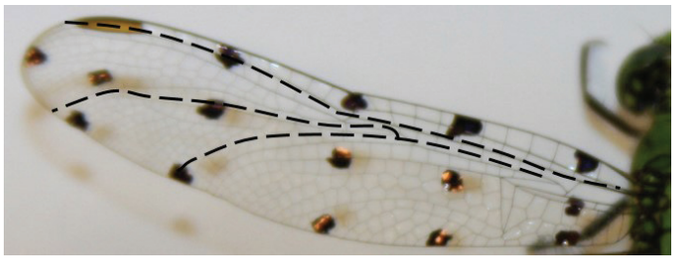

Figure 2. Sketch of the main wing veins (dashed lines) on the left forewing.

The geometrical wing shape is also of great importance in the generation of the aerodynamic force. Wing total area directly affects the magnitude of the aerodynamic force. The wing loading, defined as the ratio of the body mass over the wing area, is an indicator of flight performance. Wing area tends to increase linearly with the body dimension, whereas body mass is a function of volume increasing with the cubed body size. Therefore, insects with larger bodies usually have higher wing loading. In addition to the area, the aspect ratio, defined as the ratio of the wingspan squared to the wing area, is used to describe the wing shape. The aspect ratio of the insect wings varies in a wide range from 2 for some butterflies, to 10 for some Odonata.

Insects modulate their wing kinematics to change the aerodynamic force magnitude and direction. The body motion also affects the net movement of the wing relative to the air and therefore influences the aerodynamics of flight. In maneuvering flights, for instance, the rotation of the body can cause significant asymmetry in the trajectory of the bilateral wings. This effect is more pronounced in low-flapping-frequency insects where the rotation of the body within one wing beat is significant.

1.2. Unsteady aerodynamic of flapping wing

To achieve efficient flights in a low Reynolds number regime, insects operate their wings with a combination of translational and rotational motion in a stroke plane. The dominant unsteady flow feature that is responsible for the aerodynamic force generation is the vortex formation close to the leading edge of flapping wings. This vortical structure is produced by a laminar flow separation and produces a region of low pressure on the wing toward the leading edge. Ellington et al. [24] first illustrated a direct evidence of the existence of this leading-edge vortex (LEV) by visualizing the flow around a three-dimensional robotic wing at Reynolds number around 10^3. This unique LEV is similar to the vortical structure produced during dynamic stall observed for conventional airfoils undergoing a rapid pitch motion. However, unlike the vortex produced during a dynamic stall, the LEV is not shed even after traveling many chord lengths of distance. As the flapping wing translates in its stroke plane, a spanwise velocity gradient interacts with the LEV. This causes the axial flow to spiral toward the wing tip direction. The axial flow transported momentum out of the vortex, keeping the LEV attached and stable. The LEV began to detach at the section close to the wing tip and shed into the wake. The vortex system generated by the flapping wing induces downwash in its surrounding fluid and forms a coherent momentum jet to maintain sustained flight.

1.3. Role of wing flexibility

Flying insects typically have flexible wings to adapt to the flow environment. **Figure 3** illustrates wing deformation of different species of insects with various wing geometry and aspect ratios under various flying modes. Due to the lack of internal musculature extending into the aerodynamic surface of the wing, insects have little active control over wing deformations. Therefore, the most surface morphology of insect wings is a product of the passive mechanical properties, while flapping wings interact with the inertial and aerodynamic forces. It is widely

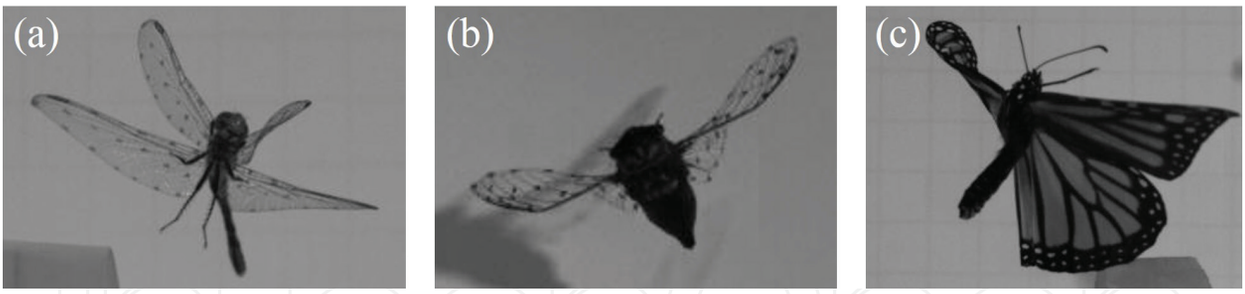

Figure 3. (a) Dragonfly in turning flight, (b) Cicada in forward flight, (c) Butterfly in takeoff flight; all showing large-scale wing deformation.

thought wing deformation would potentially provide new aerodynamic mechanisms of aerodynamic force productions over completely rigid wings in flying.

By applying either a two-dimensional foil or a highly idealized three-dimensional wing model [28–30], recent studies on the dynamic deformations during flapping flight mainly focused on the negative camber resulting from the aerodynamic and inertial forces. The development of high-speed photogrammetry has made the detailed measurements of wing deformation during high-frequency flapping motion possible. The study of deformable wing kinematics of locust [31] used a large number of marker points, and approximately 100 per wing shows that both forewings and hindwings were positively cambered on the downstroke through an "umbrella effect" whereby the trailing edge tension compressed the wing fan corrugated, reducing the projected area by 30% and releasing the tension in the trailing edge. The high-fidelity 3D dragonfly wing surface reconstruction performed by Koehler et al. [32] showed that insect wings could present up to 15% positive chordwise camber. Many fliers in nature have flexible wings which deform as the wings interact with the air around them. It has been opined that wing flexibility may provide new aerodynamic mechanisms of aerodynamic force production over completely rigid wings in flying [33–38].

1.4. Quantification of wing flexibility

The ability to capture the flight trajectory and flapping locomotion of flying insects is essential for studying flapping flight and quantifying the associated unsteady aerodynamics. Because most fliers flap too fast for the human eye to capture every detail, photogrammetry has been used to study birds [39], bats [40], and insects [41, 42].

Several previous studies have investigated the mesosurface morphological details of the wings of tethered [43, 44] and free-flying [45, 46] insects. However, these studies focused primarily on static wings. Laser scanning was used to measure the surface roughness of severed insect wings [47]. Dragonfly forewing and hindwing structures have been studied using a micro-CT scanner [48]. Corrugation in insect wings, for example, locust wings, has also been investigated [44]. However, to study corrugation, for a tethered locust, a large number of marker points (approximately 100 per hindwing) are used. Tracking these large numbers of marker points in free-flight studies is undesirable. Despite these quantitative visualizations of insect wing morphology, few works have been done on detailed measurements of 3D wing morphology

during free flight. The small wing size, fast flapping motion, and unpredictability of insect movement complicate the tracking of the details of wing kinematics and deformation.

2. In vivo insect experiments and data acquisition

In this section, a unified methodology is introduced for the surface reconstruction of insect wings during free flying motion. The currently proposed method eliminates all rigid wing assumptions while minimizing the total number of tracking points in the outputted high-speed images from the photogrammetry system. The objective is to obtain a reconstructed insect modeled to capture the details of the real insect as much as possible, which will have implications in the flight aerodynamics.

2.1. High-speed videography

Image sequences of free-flying insects are collected using three synchronized Photron Fastcam SA3 60 K high-speed cameras capable of up to 1000 frames per second at a resolution of 1024 × 1024 pixels resolution with a shutter speed of 2 μs. Three cameras are fixed on an aluminum framework, as shown in **Figure 4a**. This setup allows us to reconstruct the insects' motion in a virtual space (**Figure 4b**).The framework and foundation can ensure that cameras are aligned orthogonal to each other on an optical breadboard. The slotted channels in framework allow us to adjust the distance between cameras and insects. For providing excellent temporal and spatial resolution, the cameras are positioned 1.5 m away from the dragonfly based on the body size and flapping frequency of the specimen. The optical breadboard not only allows us to mount our hardware to a sturdy anchor but also minimizes vibrations that will occur within the system. For the lighting system, two halogen photo optic lamps (OSRAM, 54,428) are chosen for our experiment.

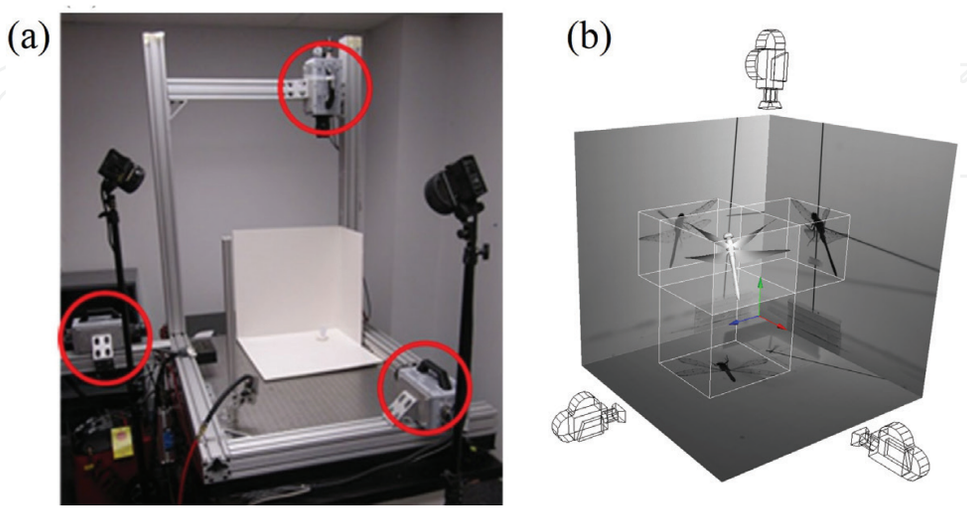

Figure 4. High-speed camera system setup in the laboratory (a) and in a virtual space (b).

After the camera system is installed, we use a daisy-chain method to loop the cameras to one another and trigger them by an external transistor-transistor logic (TTL) signal. This triggering method is an efficient way to minimize camera delay and maximize the response time. It allows us to capture images of a free-flying insect being synchronized and triggered simultaneously in three directions. The camera system can configure any standard personal computer, and the recorded sequences from the three cameras are stored locally on each camera's internal memory. All the data captured by the cameras are downloaded simultaneously to a desktop computer for subsequent analysis. The video sequences are named by using the number of cameras. Based on the quality of the image, the usable segments are identified for reconstruction.

The camera system was validated by evaluating the projection errors of filming geometries. The validation results show that there are less than 0.5 degrees in error over the entire filming data, and thus, the perspective errors can be ignored. Even though this system can minimize the human error associated with triggering the cameras, there are still some difficulties during the data collection. First, it is impossible to completely overcome the fact that the cameras are delayed from frame to frame by a small variation. Moreover, wing surface reflections caused by the lighting system sometimes make it difficult to identify the marker point clearly in the images. Since the flight paths of insects are unpredictable, capturing the true voluntary flight motion in a certain focus range of cameras is the greatest challenge.

2.2. 3D surface reconstruction

For reconstructing the wing kinematics and deformation, each insect wing is marked with a fine-tipped permanent marker before shooting the videos (e.g., a dragonfly as shown in **Figure 5a**). Since the added weight of the ink on the surface of the wing is small, we assume it is negligible and does not affect the flight performance. For an arbitrary point on a dragonfly's wing in each frame, we use the perspective projection method to decide its location in multiple projection planes. The photogrammetry system is used to capture the insect in flight.

The initial 3D wing template models are generated with Catmull-Clark subdivision surfaces by using a computer graphics software Autodesk Maya (as shown in **Figure 5b**). Based on the high-speed films, we align first-level vertices of the subdivision surface hierarchy corresponding to the marker points on insects' wings (e.g., dragonfly's forewings and hindwings). After the initial template surfaces of wings are generated, they are recorded as a keyframe animation. By repeatedly adjusting the anchor point-based alignment process along with each axis for each time step, the first level vertices of wings are completed. Although the whole process of wing reconstruction is a bit labor intensive, it is currently the only effective way to reconstruct a deformable, quad-winged insect in free flight. **Figure 6** presents the front and side views of the reconstructed wings overlapping with the corresponding high-speed images. Thus, the approximation of the 3D wing shapes such as spanwise bend, chordwise bend, and twist can be captured with smooth subdivision surface representation. Comparing with tethered insects, free-flying insects present many challenges to the surface reconstruction work due to the nonlinear translation and rotation motion, especially during turning maneuvers. **Figure 7** visualizes a reconstructed motion of the dragonfly during the free-flight maneuver at selected instants.

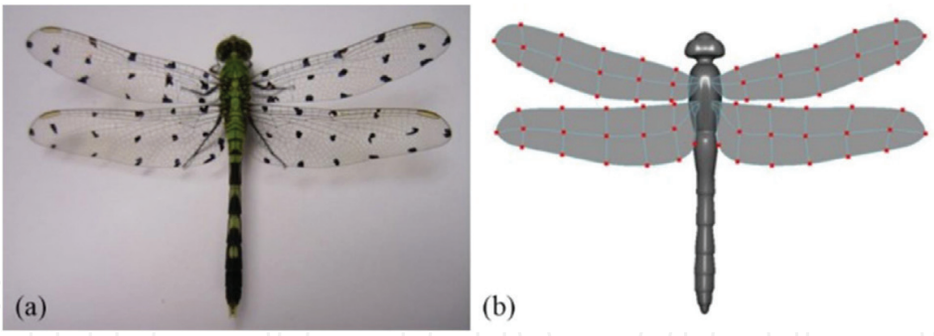

Figure 5. Initial configuration of a dragonfly template mesh. (a) Dragonfly with marker points on its wings. (b) Wing and body template models [49].

2.3. Numerical method

To study the aerodynamics of free-flight insects, the flow fields were generated by direct numerical simulations of the three-dimensional unsteady, viscous incompressible Navier-Stokes equations, as written in the following equations.

$$\frac{\partial u_i}{\partial x_i} = 0 \tag{1}$$

$$\frac{\partial u_i}{\partial t} + \frac{\partial (u_i u_j)}{\partial x_j} = -\frac{\partial p}{\partial x_i} + \frac{1}{Re}\frac{\partial}{\partial x_j}\left(\frac{\partial u_i}{\partial x_j}\right) \tag{2}$$

where u_i $(i = 1, 2, 3)$ are the velocity components in the x-, y-, and z-directions, respectively, p is the pressure, and Re is the Reynolds number.

The above Navier-Strokes equations are discretized using a cell-centered, collocated (non-staggered) arrangement, where the velocity components and pressure are located at the same physical location. The equations are then solved by using the fractional step method. The discretization of the convective terms and diffusion terms are achieved by using an Adams-Bashforth scheme and an implicit Crank-Nicolson scheme, respectively. The immersed boundary method is a computational method used to simulate fluid flow over bodies which are embedded within a Cartesian grid. It eliminates the need for the complicated re-meshing

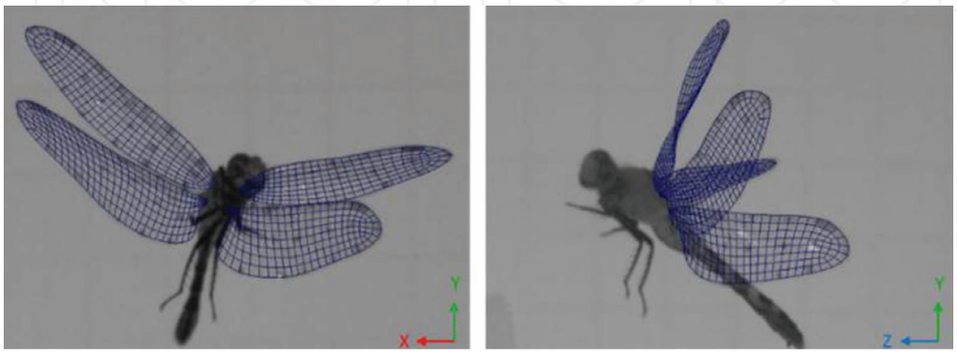

Figure 6. Reconstructed wings at a time step where a large amount of twist and camber is present in multiple wings.

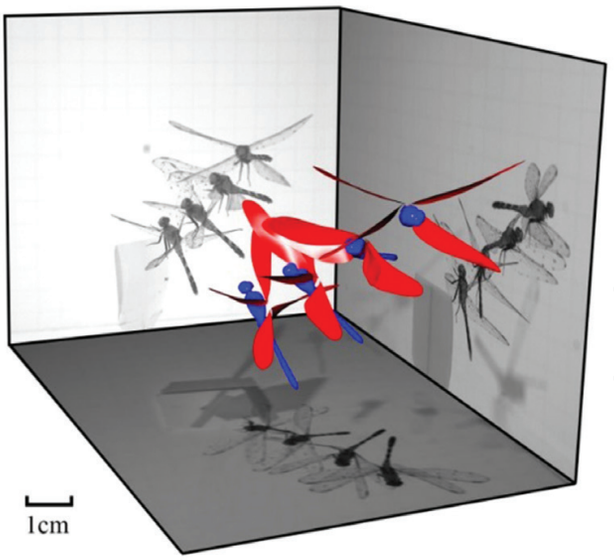

Figure 7. Motion reconstruction of dragonfly turning maneuver. The side panels show 4 of 116 frames recorded by high-speed videography [49].

algorithms and reduces the computational cost for the mesh generation in each time step that is usually employed by conventional body-conformal methods. More details for this current numerical approach can be found in [50]. The current in-house solver has also been validated by simulating canonical revolving/flapping plates [51–56], the flapping wings of insects [14, 49, 57, 58], and physiological flows [59].

3. High-fidelity analysis of flapping flight aerodynamics

In previous sections, we presented the data acquisition methods developed to obtain the most realistic reconstruction from high-speed videos. The output is a high-fidelity 3D model with the wing and body motions encoded therein. In the following discussion, the motion and deformation metrics are not isolated to study their effect on flight performance; rather, the deformations are intrinsic and influence aerodynamic footprint of the insect. Naturally, the next step is to simulate the flapping locomotion and identify the associated wake structures. We use computational fluid dynamics (CFD) simulation to understand the relevant flow features of different insects in free flight.

3.1. Dragonfly in takeoff turning flight

Dragonflies are aerial predators and feed on other flying insects. Unlike most other insects, such as flies, wasps, and cicadas, that have either reduced hindwings or functionally combined forewings and hindwings as a single pair, dragonflies have maintained two pairs of wings throughout their evolution [60]. Their neuromuscular systems allow them to individually change many aspects of wing motion in each single wing, including the angle of attack, stroke amplitude, and wing deviation, which gives them unique flying capabilities of flight control.

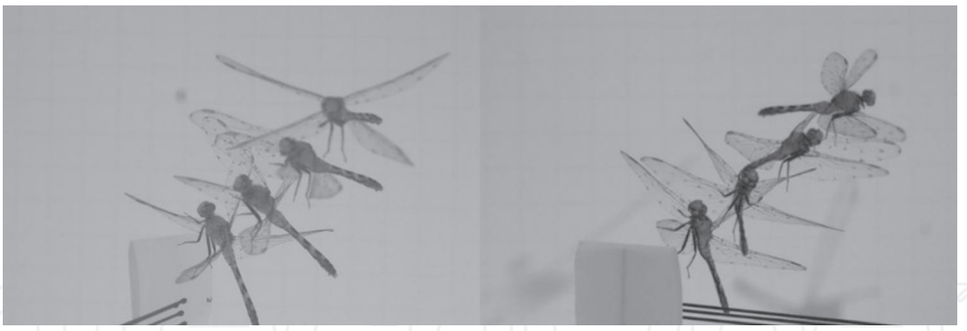

Figure 8. Snapshots of a dragonfly in takeoff turning flight from the front-view camera (left) and side-view camera (right).

In general, the flapping motion shown in **Figure 8** generates pronounced changes in the angle of attack between each side wings, especially for the forewings. During the downstroke, the magnitude of the angle of attack for the left forewing is $29 \pm 3^{\circ}$, whereas the value for the right forewing is $43 \pm 5^{\circ}$. During the upstroke, the variations of the angle of attack for the left and right forewings are $73 \pm 5^{\circ}$ and $49 \pm 3^{\circ}$, respectively. The angle of attack of the left and right hindwings at the mid-downstroke is $36 \pm 1^{\circ}$ and $21 \pm 3^{\circ}$, respectively. During the upstroke, the minimum value for the left hindwing is $23 \pm 4^{\circ}$ and for the right hindwing is $33 \pm 4^{\circ}$. For both forewings and hindwings, the asymmetric wing motion results in a relatively large angle of attack on the left-side wings during the downstroke and a small one during the upstroke. This finding implies that compared to the right-side wings, the left-side wings might experience higher drag force during the downstroke and lower thrust force during the upstroke.

Figure 9 shows the time sequence of the 3D flow field, which is identified by plotting the iso-surface of the Q-criterion [61]. To illustrate the development of the vortical structures, six snapshots from the flapping motion are shown. For each wing, a leading-edge vortex (LEV) is developed and grows stronger, remaining stably attached to the wing during the downstroke. As the wing sweeps, the LEV, the tip vortex (TV), and the shed trailing-edge vortex (TEV) connect and form a vortex loop. Because of the phase relationship between the forewings and hindwings, when the forewings reach the end of their downstroke, the hindwings have already started to move upward. As the hindwings flap upward, distinct fully developed vortex rings are gradually shed into the flow field from the trailing edge of the wings. At the same

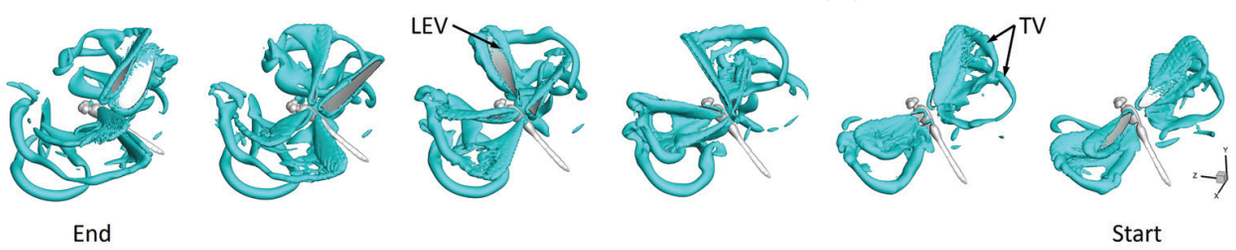

Figure 9. 3D vortex structures in the flow for a dragonfly in takeoff turning flight. The vortex structure is visualized using the iso-surface of the Q-criterion.

time, the upward-moving hindwings interact with the vortex loop formed by the forewings. This flow feature has been termed forewing-hindwing interaction in previous 2D and 3D tandem-wing studies [38, 62]. In addition to the forewing-hindwing interaction, during the upstroke, the wings catch their own wakes from the preceding downstroke, which disrupts the vortex loop structures through the wing-wake interaction and forms a stronger TV and TEV. During the maneuver, distinct asymmetric vortex formation also occurs between the left and right sides. This asymmetric phenomenon also makes the shed vortex rings tilted and distorted. By interacting with the vortex loops formed by other wings as well as previously shed vortex loops, the wake becomes more complicated. Due to the viscous dissipation effect and wing-wake interactions, only the LEV and TV in the near wake are still distinguishable in the flow field. The key features observed here are the presence of vortex loop structures in the near wake around the wings.

3.2. Butterfly in vertical takeoff

The flapping motion of a monarch butterfly (*Danaus plexippus*) in vertical takeoff flight is present in **Figure 10**. The butterfly's body and wing were then reconstructed with extraordinary details. Direct numerical simulation was then carried out in order to understand the vortex formation during the takeoff motion.

The vortex structures of the flow field are shown in **Figure 11**. Several thin swirling vortices start from each wing tip as the wings flap downward. The thin swirling vortices twist immediately after the separation from each wing tip and form a tip vortex (TV) during the downstroke. As the butterfly left upward, the thin vortices are merged by the viscosity into a coherent vortex under the insect body. The TV during downstroke generates lift as the reaction of inducing the downward flow. Wingtip vortices during upstroke are also made by the vorticities of the wings aligned close to the negative and positive vertical directions. Trailing-edge vortices released at the transitions from downstroke to upstrokes are barely visible in the wake of butterfly flapping motion.

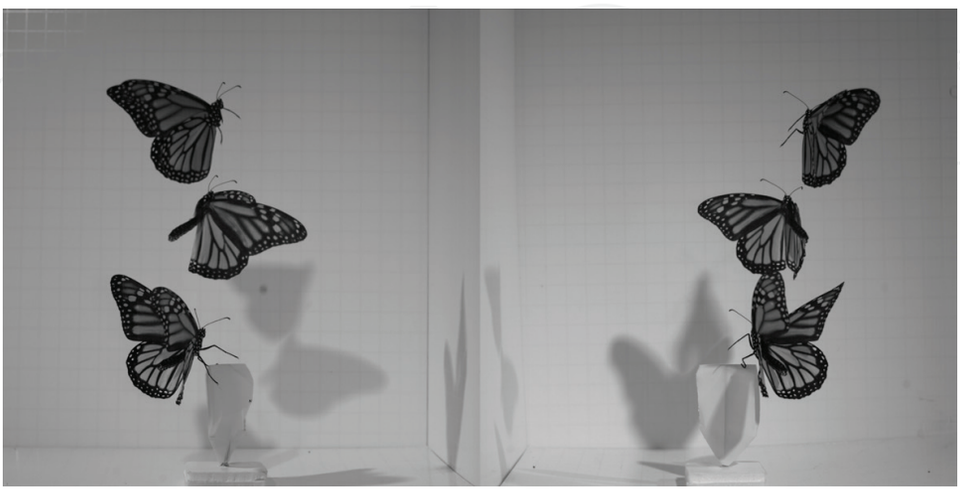

Figure 10. Snapshots of a butterfly in takeoff flight from the front-view camera (left) and side-view camera (right).

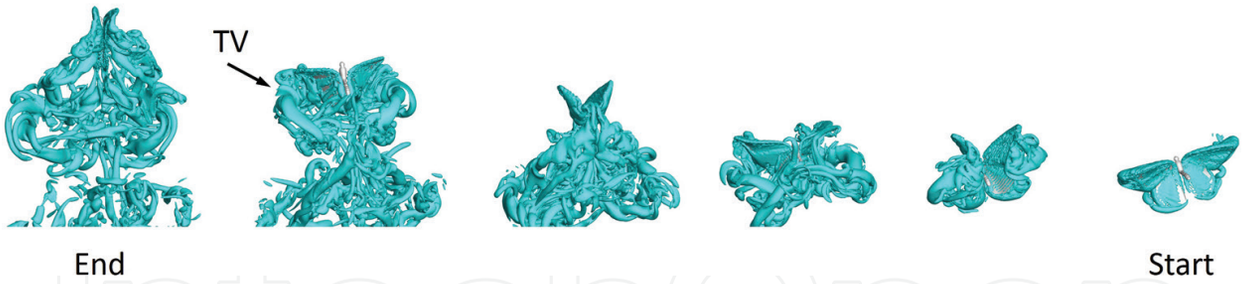

Figure 11. 3D vortex structures in the flow for a butterfly in takeoff flight. The vortex structure is visualized using the iso-surface of the Q-criterion.

3.3. Damselfly in yaw turn

Here, a damselfly (*Calopteryx maculata*) is involved in performing a yaw turn maneuver during which it also ascends for about three body lengths (**Figure 12**). To perform a turning maneuver, the wings must generate aerodynamic forces to sustain body weight while simultaneously producing turning moments to rotate the body around its center of mass (CoM) while remaining almost-stationary or moving forward. During a yaw turn, the horizontal component of the aerodynamic force is oriented toward the center of curvature. This force reorientation produces lateral forces for rotation around the center of mass. In addition, an asymmetry in wing kinematics between the wings on the outside of the turn (left wings) and right wings on the inside of the turn is necessary to create a yaw torque differential. Insights into how the damselfly flight forces can be gleaned from the flow field data. To generate forces for flight, the damselfly used an unsteady mechanism such as a leading-edge vortex on its wings which feeds into a tip vortex (**Figure 13**). Although the wake structure is quite complex, an asymmetric flow structure with a stronger flow field oriented toward the right wing is observed, which indicates that the inner wings may be playing a substantial role in executing the turn by creating large force/yaw torque differences between the contralateral wing pairs.

Figure 12. Snapshots of a damselfly in yaw turn from the top-view camera (left) and side-view camera (right).

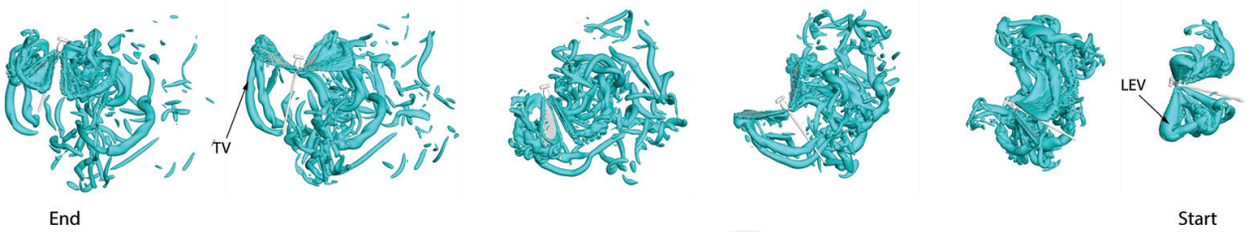

Figure 13. 3D vortex structures in the flow for a damselfly in yaw turn. The vortex structure is visualized using the iso-surface of the Q-criterion.

3.4. Cicada in turning maneuver

Here, the flight of a cicada which initiates flight and immediately executes a banked turn is recorded. Unlike the yaw turn scenario of the damselfly where the wings do the majority of the force reorientation, and the roll motion of the body is minimal, banked turns are distinct but more commonly found in nature. During banked turns, the animal reorients the total aerodynamic force vector toward the center of the turn by simply rotating the body around its longitudinal axis. This is evident in **Figure 14** wherein the cicada rolls its body by about 90° to reorient the force vector into the center of curvature like an airplane. During this flight, the cicada still utilizes unsteady mechanism such as a LEV (**Figure 15**) to help maintain a strong enough component to sustain weight. The asymmetry in flow features on the left and right sides indicates a force difference necessary to induce a roll torque for the turn.

Figure 14. Snapshots of a cicada in takeoff turning flight from the front-view camera (left) and side-view camera (right).

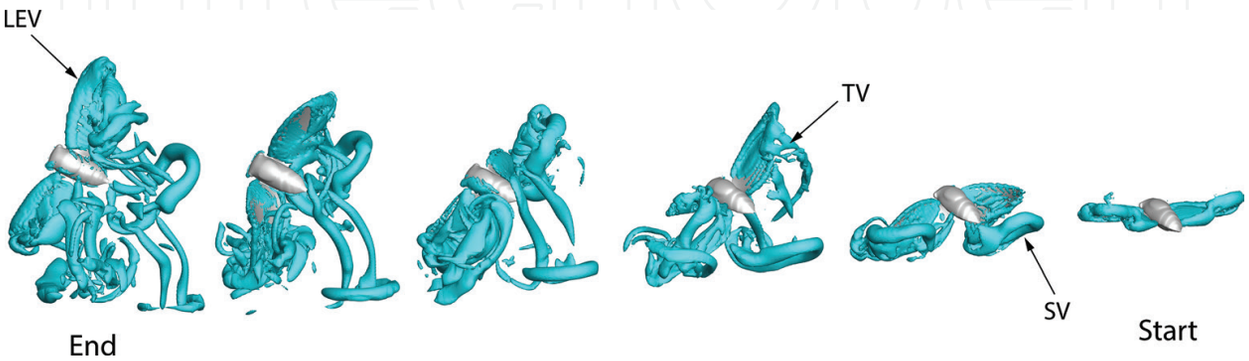

Figure 15. 3D vortex structures in the flow for a cicada in takeoff turning flight. The vortex structure is visualized using the iso-surface of the Q-criterion.

4. Conclusion

In the current chapter, we present an integrative approach to study the aerodynamics of free-flying insects. This proposed novel approach combines high-speed photogrammetry, 3D surface reconstruction, and computational fluid dynamics and is capable of measuring the wing kinematics and surface deformation and simulating its aerodynamic performance. Four different species of insects, including dragonfly, damselfly, butterfly, and cicada, were investigated to demonstrate the capability of the current method. From these collected data, we provide insight into the understanding of flapping wing mechanism and revealing the underlying flow physics for future MAV designs and applications.

Acknowledgements

This research is supported by NSF grant CBET-1313217 and AFOSR grant FA9550-12-1-0071. We thank former members of Flow Simulation Research Group at Wright State University and University of Virginia for capture of highspeed videos. We thank Yan Ren for **Figure 4(b)**.

Author details

Haibo Dong*, Ayodeji T. Bode-Oke and Chengyu Li

*Address all correspondence to: haibo.dong@virginia.edu

Mechanical and Aerospace Engineering, University of Virginia, Charlottesville, VA, USA

References

[1] Weis-Fogh T, Jensen M. Biology and physics of locust flight. i. Basic principles in insect flight. A critical review. Philosophical Transactions of the Royal Society of London Series B: Biological Sciences. 1956;**239**:415-458

[2] Dudley R. The Biomechanics of Insect Flight. Princeton: Princeton University Press; 2000

[3] Weisfogh T. Quick estimates of flight fitness in hovering animals, including novel mechanisms for lift production. Journal of Experimental Biology. 1973;**59**:169-230

[4] Lighthill MJ. On the Weis–Fogh mechanism of lift generation. Journal of Fluid Mechanics. 1973;**60**:1-17

[5] Ellington CP. The aerodynamics of hovering insect flight. 3. Kinematics. Philosophical Transactions of the Royal Society of London Series B: Biological Sciences. 1984;**305**:41-78

[6] Maxworthy T. Experiments on the Weis–Fogh mechanism of lift generation by insects in hovering flight Part 1. Dynamics of the 'fling'. Journal of Fluid Mechanics. 1979;**93**:47-63

[7] Ellington CP. Unsteady aerodynamics of insect flight. Symposia of the Society for Experimental Biology. 1995;**49**:109-129

[8] Dickinson MH, Lehmann FO, Sane SP. Wing rotation and the aerodynamic basis of insect flight. Science. 1999;**284**:1954-1960

[9] Birch. Investigation of the near-field tip vortex behind an oscillating wing. Journal of Fluid Mechanics 2005;**544**:201-241

[10] Maxworthy T. The fluid-dynamics of insect flight. Annual Review of Fluid Mechanics. 1981;**13**:329-350

[11] van den Berg C, Ellington CP. The vortex wake of a 'hovering' model hawkmoth. Philosophical Transactions of the Royal Society of London Series B: Biological Sciences 1997;**352**:317-328

[12] Sane SP, Dickinson MH. The aerodynamic effects of wing rotation and a revised quasi-steady model of flapping flight. The Journal of Experimental Biology. 2002;**205**:1087-1096

[13] Sun M, Tang J. Unsteady aerodynamic force generation by a model fruit fly wing in flapping motion. The Journal of Experimental Biology. 2002;**205**:55-70

[14] Liu G, Dong H, Li C. Vortex dynamics and new lift enhancement mechanism of wing–body interaction in insect forward flight. Journal of Fluid Mechanics. 2016;**795**:634-651

[15] Anderson JM, Streitlien K, Barrett DS, Triantafyllou MS. Oscillating foils of high propulsive efficiency. Journal of Fluid Mechanics. 1998;**360**:41-72

[16] Shyy W, Berg M, Ljungqvist D. Flapping and flexible wings for biological and micro air vehicles. Progress in Aerospace Sciences. 1999;**35**:455-505

[17] Platzer MF, Jones KD, Young J, Lai JCS. Flapping-wing aerodynamics: Progress and challenges. AIAA Journal. 2008;**46**:2136-2149

[18] Jones K, Dohring C, Platzer M. Wake structures behind plunging airfoils: A comparison of numerical and experimental results. AIAA Paper 1996-0078:1996

[19] Wu JZ. Theory for aerodynamic force and moment in viscous flows. AIAA Journal. 1981;**19**:432-441

[20] Noca F, Shiels D, Jeon D. A comparison of methods for evaluating time-dependent fluid dynamic forces on bodies, using only velocity fields and their derivatives. Journal of Fluids and Structures. 1999;**13**:551-578

[21] Wu JZ, Ma HY, Zhou MD. Vorticity and Vortex Dynamics. Berlin Heidelberg New York: Springer; 2006

[22] Ho S, Nassef H, Pornsinsirirak N, Tai YC, Ho CM. Unsteady aerodynamics and flow control for flapping wing flyers. Progress in Aerospace Sciences. 2003;**39**:635-681

[23] Tijdeman H, Seebass R. Transonic flow past oscillating airfoils. Annual Review of Fluid Mechanics. 1980;**12**:181-222

[24] Ellington CP, van den Berg C, Willmott AP, Thomas ALR. Leading-edge vortices in insect flight. Nature 1996;**384**:626-630.

[25] Dudley R. The Biomechanics of Insect Flight: Form, Function, Evolution. Princeton: Princeton University Press; 2002

[26] Ellington CP. The aerodynamics of hovering insect flight. 1. The quasi-steady analysis. Philosophical Transactions of the Royal Society of London Series B: Biological Sciences. 1984;**305**:1-15

[27] Betts C, Wootton R. Wing shape and flight behaviour in butterflies (Lepidoptera: Papilionoidea and Hesperioidea): A preliminary analysis. The Journal of Experimental Biology. 1988;**138**:271-288

[28] Chimakurthi SK, Tang J, Palacios R, Cesnik CES, Shyy W. Computational aeroelasticity framework for analyzing flapping wing micro air vehicles. AIAA Journal. 2009;**47**:1865-1878

[29] Hamamoto M, Ohta Y, Hara K, Hisada T. Application of fluid-structure interaction analysis to flapping flight of insects with deformable wings. Advanced Robotics. 2007;**21**:1-21

[30] Yin B, Luo HX. Effect of wing inertia on hovering performance of flexible flapping wings. Physics of Fluids. 2010;**22**:111902

[31] Walker SM, Thomas ALR, Taylor GK. Deformable wing kinematics in the desert locust: How and why do camber, twist and topography vary through the stroke? Journal of the Royal Society Interface. 2009;**6**:735-747

[32] Koehler C, Liang ZX, Gaston Z, Wan H, Dong HB. 3D reconstruction and analysis of wing deformation in free-flying dragonflies. The Journal of Experimental Biology. 2012;**215**:3018-3027

[33] Wootton RJ. Leading edge section and asymmetric twisting in the wings of flying butterflies (Insecta, Papilionoidea). The Journal of Experimental Biology. 1993;**180**(1):105-117

[34] Combes SA, Daniel TL. Shape, flapping and flexion: wing and fin design for forward flight. Journal of Experimental Biology. 2001;**204**(12):2073-2085

[35] Combes SA, Daniel TL. Flexural stiffness in insect wings. I. Scaling and influence of wing venation. Journal of Experimental Biology. 2003;**206**:2979-2987

[36] Combes SA, Daniel TL. Flexural stiffness in insect wings. II. Spatial distribution and dynamic wing bending. Journal of Experimental Biology. 2003;**206**:2989-2997

[37] Sane SP. The aerodynamics of insect flight. Journal of Experimental Biology 2003;**206**(23): 4191-4208

[38] Lehmann FO. When wings touch wakes: Understanding locomotor force control by wake-wing interference in insect wings. The Journal of Experimental Biology. 2008;**211**:224-233

[39] Tobalske BW, Warrick DR, Clark CJ, Powers DR, Hedrick TL, Hyder GA, et al. Three-dimensional kinematics of hummingbird flight. The Journal of Experimental Biology. 2007;**210**:2368-2382

[40] Norberg UML, Winter Y. Wing beat kinematics of a nectar-feeding bat, *Glossophaga soricina*, flying at different flight speeds and Strouhal numbers. The Journal of Experimental Biology. 2006;**209**:3887-3897

[41] Ristroph L, Berman GJ, Bergou AJ, Wang ZJ, Cohen I. Automated hull reconstruction motion tracking (HRMT) applied to sideways maneuvers of free-flying insects. The Journal of Experimental Biology. 2009;**212**:1324-1335

[42] Liu YP, Sun M. Wing kinematics measurement and aerodynamics of hovering droneflies. The Journal of Experimental Biology. 2008;**211**:2014-2025

[43] Sunada S, Song D, Meng X, Wang H, Zeng L, Kawachi K. Optical measurement of the deformation, motion, and generated force of the wings of a moth. JSEM International Journal. 2002;**45**(4):836-842

[44] Walker SM, Thomas ALR, Taylor GK. Photogrammetric reconstruction of high-resolution surface topographies and deformable wing kinematics of tethered locusts and free-flying hoverflies. Journal of the Royal Society Interface. 2009;**6**:351-366

[45] Bergou AJ, Ristroph L, Guckenheimer J, Cohen I, Wang ZJ. Fruit flies modulate passive wing pitching to generate in-flight turns. Physical Review Letters. 2010;**104**:141801

[46] Walker SM, Thomas ALR, Taylor GK. Deformable wing kinematics in free-flying hoverflies. Journal of the Royal Society Interface. 2010;**7**:131-142

[47] Sudo S, Tsuyuki K, Kanno K. Wing characteristics and flapping behavior of flying insects. Experimental Mechanics. 2005;**45**:550-555

[48] Jongerius SR, Lentink D. Structural analysis of a dragonfly wing. Experimental Mechanics. 2010;**50**:1323-1334

[49] Li C, Dong H. Wing kinematics measurement and aerodynamics of a dragonfly in turning flight. Bioinspiration & Biomimetics. 2017;**12**:026001

[50] Mittal R, Dong H, Bozkurttas M, Najjar FM, Vargas A, von Loebbecke A. A versatile sharp interface immersed boundary method for incompressible flows with complex boundaries. Journal of Computational Physics 2008;**227**:4825-4852.

[51] Li C, Dong H. Three-dimensional wake topology and propulsive performance of low-aspect-ratio pitching-rolling plates. Physics of Fluids. 2016;**28**:071901

[52] Xu M, Wei M, Li C, Dong H. Adjoint-based optimization of flapping plates hinged with a trailing-edge flap. Theoretical and Applied Mechanics Letters. 2015;**5**:1-4

[53] Wan H, Dong H, Li C, Liang Z. Vortex formation and aerodynamic force of low aspect-ratio plate in translation and rotation. AIAA Paper 2012-3278; 2012

[54] Li C, Dong H. Wake structure and aerodynamic performance of low aspect-ratio revolving plates at low Reynolds number. AIAA Paper 2014-1453; 2014

[55] Li C, Dong H, Liang Z. Proper orthogonal decomposition analysis of 3-D wake structures in a pitching-rolling plate. AIAA Paper 2016-2071; 2016

[56] Li C, Dong H, Cheng B. Effects of aspect ratio and angle of attack on tip vortex structures and aerodynamic performance for rotating flat plates. AIAA Paper 2017-3645; 2017

[57] Li C, Wang J, Dong H. Proper orthogonal decomposition analysis of flapping hovering wings. AIAA Paper 2017-0327; 2017

[58] Wang J, Li C, Ren Y, Dong H. Effects of surface morphing on the wake structure and performance of flapping plates. AIAA 2017-3643; 2017

[59] Li C, Jiang J, Dong H, Zhao K. Computational modeling and validation of human nasal airflow under various breathing conditions. Journal of Biomechanics. 2017;**64**:59-68

[60] Bomphrey RJ, Nakata T, Henningsson P, Lin H-T. Flight of the dragonflies and damselflies. Philosophical Transactions of the Royal Society of London Series B: Biological Sciences. 2016;**371**:20150389

[61] Hunt JCR, Wray AA, Moin P. Eddies, streams, and convergence zones in turbulent flows. Center for Turbulence Research Report CTR-S88; 1988:193-208

[62] Wang J, Russell D. Effect of forewing and hindwing interactions on aerodynamic forces and power in hovering dragonfly flight. Physical Review Letters. 2007;**99**:148101